Examination of the Physics solution of COVID-19

To cite this article: T.J. Abodunrin and M.E. Emetere 2022 *IOP Conf. Ser.: Earth Environ. Sci.* **993** 012011

Examination of the Physics solution of COVID-19

T.J. Abodunrin[1] and M.E. Emetere[1]

[1]Department of Physics, Covenant University, Ota, Ogun State, Nigeria

Corresponding author (T.J. Abodunrin):
temitope.abodunrin@covenantuniversity.edu.ng; Orcid: 0000-0001-9109-277X

(M.E. Emetere): moses.emetere@covenantuniversity.edu.ng; Orcid: 0000-0002-2968-8676

Abstract. The Viruses are pathogens capable of infecting more than 10% of the world's population annually in epidemics responsible for 3 to 5 million cases of severe illness and up to 500 000 deaths. In addition, new virus variants pose a continuous threat of sparking pandemic outbreaks. The success of the viral attack is attributed to their sheath in a capsid, abnormal mass production of infective RNA or DNA genetic material in living target. Other features include, great symmetry in structures based on assorted geometries with amazing mechanical properties. Consequently, prognostic models have been deployed to regulate and unravel understanding for successful treatment of viruses. In particular, this report seeks to investigate SARS-CoV-2 through its viral shell mechanical properties and a novel point of entropy and thermodynamic principles. It concludes with recommendation of effective physical remedies for SARS-CoV-2 from a local and global outlook.

Keywords: COVID-19, SEIR model, SELIHARD model, Thermodynamics, Sonic therapy.

1. Introduction

As the shock waves of COVID contagion still reverberates around the globe, an anti-epidemic battle rages on [1]. Consideration of the viral rudimentary duplication, time for replication and consecutive interval of each viral stage necessitates statistical models. Arguably, COVID solution is strictly either medical or biological however, theoretical studies based on mathematical modelling serve as indicators [2]. Their significance ranges from preliminary determination of epidemic outbreak physiognomies, predicting the modulation and termination points in mitigating the spread [3]. Mathematical modelling dynamical equations actually provide more detailed insights into the underlying forces of the epidemic. The regular susceptible exposed infectious recovered (SEIR) model is the most extensively embraced for characterizing the COVID-19 epidemic in China and other countries as shown in Figure 1 [4]. Analysis of the COVID contagion based on the conventional SEIR model uses seven classic states. They are described as {E(t), S(t), P(t), I(t), Q(t), R(t), D(t)} representing total cases of exposed cases; susceptible cases, insusceptible cases, infectious cases, quarantined cases, recovered cases and death respectively. A version of the SEIR model is as summarized in Figure 2 [5].

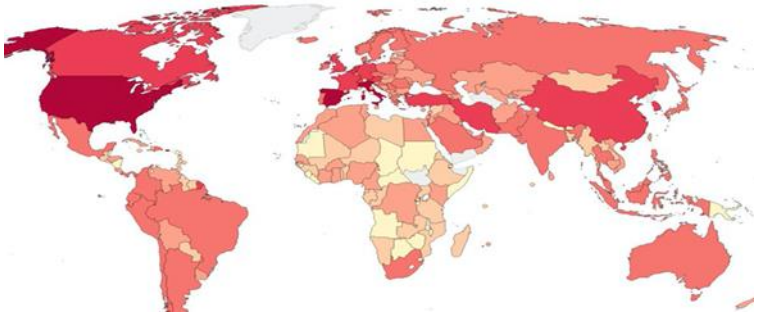

Figure 1: Word Cloud of Countries in the World with higher index cases of COVID-19

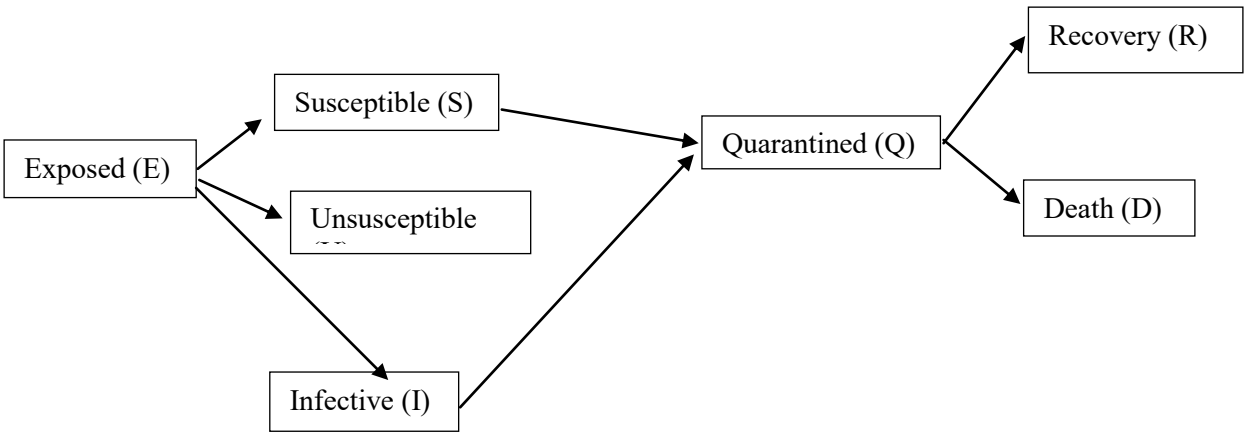

Figure 2: Revised SEIR model [6]

Some notable exceptions to the SEIR evaluation model were found in the subsect of persons either quarantined or not quarantined. Consequently, statistical methods became sorely tried in trying to assess the effectiveness of each method. In response to this situation, torrents of SEIR models were adapted to mimic transmission, source contagion, capsid storage and variations in prey. This further led to a rise in extensions to the classical SEIR model which was specifically to address routine delays, such as the interval during incubation and time for recovery. A peculiar challenge still arose, pioneer models were either too complex thus, they did not prescribe solutions to the overfitting problem. Nor were the factors estimated based on sufficient and precise data, obviously giving rise to doubtful prognoses. However, due to the lack of official data and the change of diagnostic calibre during the early stage of the outbreak. Inspired by these reasons, another model, a SELIAHRD model is prescribed. It comprises eight compartments, {Susceptible, Exposed, Latent, Symptomatic/Infected, Asymptomatic, Hospitalized, Recovered, and Death}. This is due to an addition- the latent compartment, this includes the people which can be classified as symptomatic and asymptomatic people. SELIAHRD model, shown in Figure 3 reckons with patients with mild cases of COVID 19 symptoms which are responsible for the spike in cases in many countries. A revision to the SELIAHRD model reasoning is that, exposure to the contagion is responsible for the susceptibility as indicated by Figure 3. Symptoms latent or otherwise, are

classified as symptomatic or asymptomatic. Asymptomatic are treated as outpatients while symptomatic ones get hospitalized, some recover and are discharged, others who do not recover die. There are a number of cases reported by world health organization (WHO) that show a deviation from this pattern due to underlying health complications described by medical standard practices. The latent state also has a probability of either being positive or negatively contagious as a hypothesis. Laboratory tests affirm the validity of this idea, in which case, the prognosis [7]. In this work, we discuss the effect of introducing a new quarantined state, authentic cures, preventive measures, key factors; such as latent time, quarantine time and effective reproduction number in a comparative way. Mathematical interpretation of inflection point, ending time and total infected cases in 228 regions are used to predict and validate some direct and indirect evidences. In view of continuous revisions to combat resistant strains of COVID -19 and a re-infection of already vaccinated people, the analysis of affected countries is still in progress. A multi-dimensional effort is expressed simultaneously through biotechnology, medicine, nanotechnology, drug application, thermodynamic principles. They all remotely working on evolving a novel drug design adept from hijack of subsequent viral insurgent is the future prescribed in this study [8].

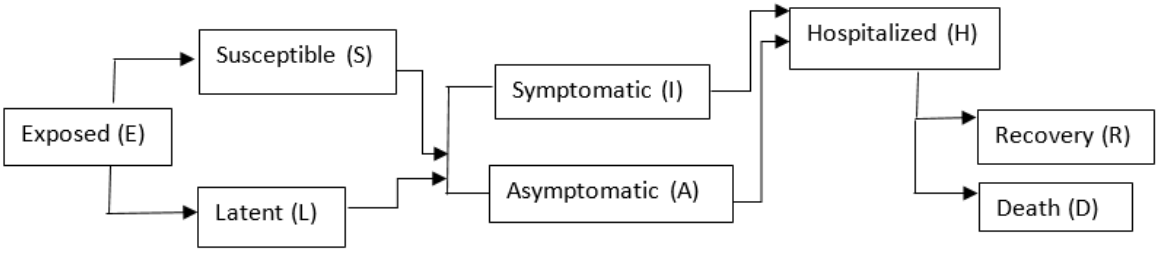

Figure 3: Revised SELIAHRD Model [9]

Background Theory

A general model for viral replication dynamics is given by Equation 1. Where λ represents the total number of cells before infection, they die normally at rate of dn , vulnerable uninfected cells, *n(t),* are infected when they meet free viruses, *v(t).* They get infected at a rate of βnv, as denoted by Equation 2, this results in infected cells, *y(t),* producing new virus particles at a rate *ky*. Infected cells multiply at thatk/(d + α), infected viruses' decay *uv* as given by Equation 3 [10].

$$\frac{dy}{dn} = \lambda - dn - \beta nv \quad (1)$$

$$\frac{dy}{dt} = \beta nv - (d + \alpha)y \quad (2)$$

$$\frac{dv}{dt} = ky - uv \quad (3)$$

The consequence of Equations 1-3, i.e. infection, reproduction and death determine the number of incidences within a time frame. Immunity of a host cell symbolizes an energy barrier any virus, or COVID-19 needs to overcome, each viral attack is a probability function

of this failure or success. Energetic viruses have a higher probability of surmounting the potential barrier of the host immunity. One method of overcoming this barrier is by using temperature increase in the viral system, these two parameters are represented by Arrhenius equation for temperature dependent reaction, Equation 4. S successful viral attempts must be $\geq e_i = exp\left(f_i/T\right)$, e_i represents probability of success and T signifies temperature of the system. Although one of the most abiotic factor that affects any ecosystem, susceptibility and sensitivity are the key factors that describe viral reproduction or annihilation with change in temperature. Results suggest that whilst the rank order of species susceptibilities may remain the same with changes in temperature, some species may become more susceptible to a novel pathogen, and others less so.

$$ln\,K = l\,n\,A - e^{-(Ea/RT)} \qquad 4$$

In Equation 4, as Temperature (K) increases, $\frac{Ea}{RT}$ decreases, -$\frac{Ea}{RT}$ increases where E_a is the activation energy, *RT* is average kinetic energy and *K* is viral load constant. When A, pre-exponential factor is a small value, entropy decreases smoothly and continuously as temperature is raised. This explains viral sensitivity, the ability of a virus to either multiply below par or not at all, at body temperature. Temperature sensitivity thus influences the constraint of the infection to respiratory pathways, reducing the probability of systemic infection and the range of the viral attack. In the event of a minor respirational ailment coupled with an inadequate immune response relative to the systemic infection, re-infection may occur later. At high values of A, entropy fluctuates to the normal body temperature of the host, a temperature zone where viruses replicate poorly are less virulent than those that can replicate freely at body temperature. The Boltzmann's constant is introduced to obtain the universal product as shown in Equations 5 to 7.

$$P = \prod_{j=1} P_j = \prod j = 1\left[\pi N_k\, e^{-\Delta Gjk/K_BTe} + i\Delta Q_{jk}/K_BT\right] N_j/N_j\,! \qquad 5$$

In this way, entropy is regarded as logarithm of *P* as expressed in Equation 6.

$$S = K_B[ln_{j=1}(\pi_{k=1} N_k\, e^{-\Delta Gjk/K_BTe} + i\Delta Q_{jk}/K_BT)^{N_j}/N_j! \qquad 6$$

$$S = \frac{1}{T}\left[\sum_{j=1} N_j K_B T + N_j\left(\sum_{k=1} \mu_k - \mu_j + i\Delta Q_{jk}\right)\right] \qquad 7$$

Results and Discussion

A plot of COVID-19 incidences obtained from database is as shown on Table 1, this revealed Figure 4. The figures were in turn used to obtain information on the prototype of behavioural pattern across the 228 countries considered over time. Six distinct characteristics: A, B, C, D, E and F were identified. Type D was the most predominant, while E was least in occurrence.In order to discuss the inflexion parameters, each graph would be considered as a point of ½ symmetry.

Table 1: Classification of 228 World Countries according to graphical prototype

A		B	C	D	E	F
Aruba$_c$,Andorra AUS$_e$, CHN, BFA, BRB$_c$, BRN, CHE, CRI, CZE$_e$, DEU, ERI$_c$, ESP, EST, FRO, GIB$_c$, GRC$_d$, HRV, IMN$_d$, ISL$_d$, ISR, ITA$_e$, JEY$_c$, JOR, KHM$_c$, KNA$_c$, KOR, LBN$_d$, LCA$_c$, LIE$_c$, LUX, MDG$_c$, KCL$_c$, ISL$_d$, ISR, ITA$_e$, JEY$_c$, JOR, KHM$_c$, KNA$_c$, KOR, LBN$_d$, LCA$_c$, LIE$_c$, LUX, MDG$_c$, KCL$_c$, NER$_c$, NZL, PYF$_c$, SVN$_d$, SXM$_c$, TGA, TTO$_c$, TWN$_d$, VNM$_d$		Afghanistan, Angola, ARE, ARG$_d$, BGD, BLR, BOL, BRA, CAN, CHL, COL, ECU$_c$, DOM, GAB$_c$, GUM, IND, IRQ$_d$, JPN, KAZ$_d$, KWT, MAR, MDA, MDV, MEX, MKD$_d$, NGA, NPL$_c$, OMN, PAK, PER, QAT, RUS, SAU, SDN, SGP, SOM, SWE, SWZ$_c$, TCD$_c$, UKR, ZAF	Anguilla, ATG, BDI, BEN, BES, BLZ, BMU$_d$, BTN$_a$, BWA$_a$, CMR$_d$, COG, CPV, CUW, CYM$_a$, DMA$_a$, ECU$_d$, COG$_a$, ERI, FJI$_a$, FLK, GMB, GNB, GNQ, GRD, GRL, GUY$_d$, HTI$_d$, LAO, LBY, MNG, MNP, MOZ, MRT, MSR, MWI, NAM$_a$, NIC, PNG, PSE, SSD, STP, SUR, SYC, SYR, TCA, UGA, VAT, VCT, VGB, VIR	Albania, ARM, BEL, BGR, BHR$_b$, BHS, BIH, CIV, COD, COL, CAF$_c$, CAN$_b$ CUB, DNK, DOM, DZA, ETH, FIN, GBR, GEO, GGY$_a$, GHA$_c$, GIN$_b$, GTM, HND, HUN, IDN, IRA$_a$, IRN$_a$, JAM, KEN, KGZ$_c$, LBR, LKA, LTU$_c$, LVA, MCO$_a$, MLI$_b$, MLT$_a$, MMR$_a$, MNE$_a$, MUS, MYS, NLD, PAN, PHL, POL, PRI, PRT, PRY, RKS, ROU, RWA$_c$, SEN, SLE, SLV, SMR, SRB, SVK, TGO$_c$, TUN, TUR, TZA$_c$, URY, USB, VEN$_c$, ZMB$_c$,	**AUT$_a$**, AZE, CYP$_a$, DJI, FRA$_a$, NOR	COM, ESH, HKG, TKK$_d$, TLS$_a$, USA$_d$, YEM$_c$
Subtotal:	56	**41**	**50**	**68**	**6**	**7**

The viral loads are given as; 10, 21, 7, 13, 13 and 0 days respectively, the subsequent peak indicates the rate of infections which is highest in type B, with 2,500 cases in 57 days. Recovery rate was largely due to number of testing and swift isolation and treatment of patients as indicative in types F and C.

Type A

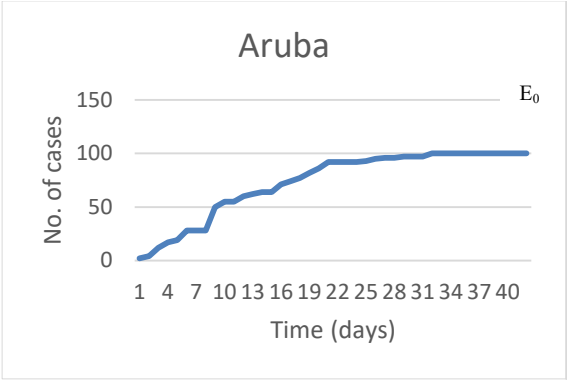

Type B

Type C

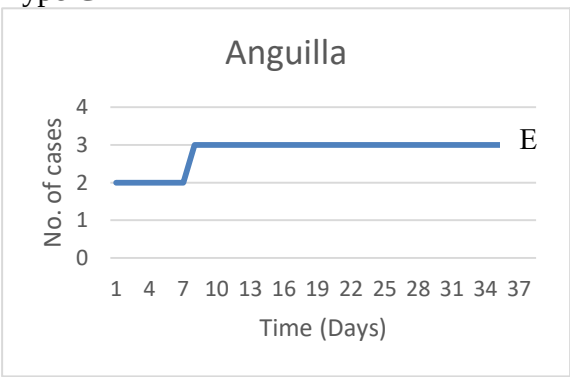

Type D

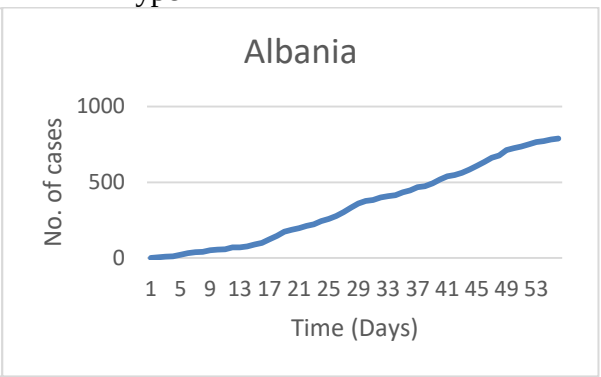

Type E

Type F

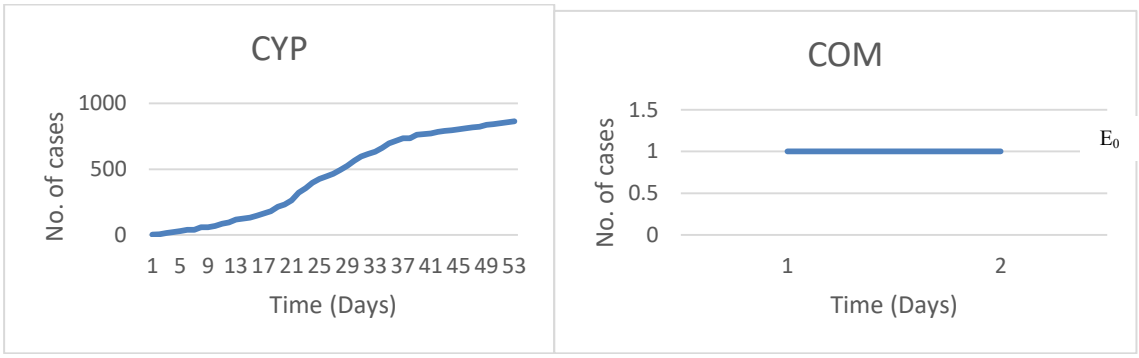

Figure 4: Graphical representation of COVID-19 cases in 228 Countries.

A Physics Interpretation of Graphical Responses

From Figure 4 (a)-(f), 228 Countries considered, in terms of entropy and infection, outcomes can be classified under two broad groups:S_0< 1, one cell averagely produced less than one new infected cell, the viruspopulation nosedives and becomes defunct, resulting in an infection-free system. This is typical of Type C and F Countries as shown on Table 1, the viral infection has attained an equilibrium E_0. Conversely, when S_0> 1, represents a condition where one cell averagely gives rise to more than one newlyinfected cell, and the viral infection can spread quickly until the system converges to attain a positive equilibrium, this is the case in Country Type A. There is a variant of S_0> 1, this describes a situation when the viral infection is rapidly spreading and the equilibrium position is yet to be attained, an illustration of this is given by Country Types B, D and E. The graphic picture of a Viral model as shown in Figure 5 [20] corroborates with the different types of COVID-19 presentations in Figure 3. In the model, *(T)* stands for susceptible target cells, (*I*) represents viral producing cells and (*V*) connotes the virus load. Type *A* and *B* graphs coincides with points *K* and *P* respectively on the viral model whereas Types C, D, E and F are linear representations of Graphs A and B. Graph B is an illustration of a P-V diagram.

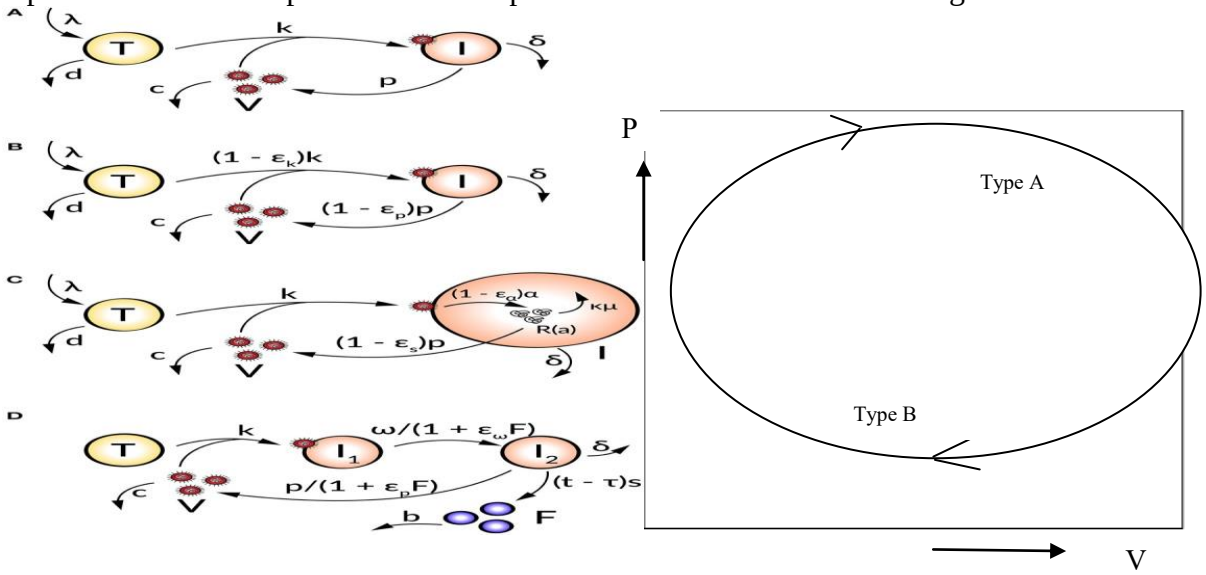

Figure 5: Comparison of Viral model and thermodynamic cyclic process [11]

The P-V interrelationship link the viral pattern of behaviour to a thermodynamic theory, Table 2 is used to present these associations. The work done (W) by the virus is described by its replication in Equation 8 and 14. Rate of infection (I) is explained by the change in energy or entropy given by Equations 9 and 15. The effect of this multiplicity factor is as denoted by a change in volume, dv which gives rise to change in the internal energy of the host, termed COVID-19 as shown in Equations 10, 16 and 17. A specific application of thermodynamic application to anti-viral therapy is akin to an ideal situation, i.e. before the viral insurgence given as Equations 10-13 and 18-20.

Table 2: A representation of Mathematical Vs Thermodynamic model

Mathematical Model		**Thermodynamical Model**	
$\frac{dT}{dt} = \boldsymbol{\lambda - dT - KVT}$	**8**	$W = pdV$	14
$\frac{dI}{dt} = \boldsymbol{KVT - \delta I}$	**9**	$dQ = SdT$	15
		$dU = dQ - dW$	16
		$dU = SdT - pdV$ 17	
$\frac{dv}{dt} = \boldsymbol{PI - cV}$	**10**	Ideal-Gas Condition:	
Anti-viral therapy:		$\frac{dS}{dt} \geq 0$	18
$\frac{dT}{dt} = \boldsymbol{\lambda - dT - (1 - \varepsilon_k)KVT}$	**11**	$\frac{dT}{dt} > 0; P_{const.} = \frac{dV}{dt} > 019$	
$\frac{dI}{dt} = \boldsymbol{(1 - \varepsilon_k)KVT - \delta I}$	**12**	$\frac{dP}{dt} > 0;\ V_{const.} = \frac{dT}{dt} > 0$	20
$\frac{dv}{dt} = \boldsymbol{(1 - \varepsilon_k)\ PI - cV}$	**13**		

Exploring the effect of pressure by COVID-19 in a patient is indicated in Equation 20, this suggests that blood pressure of patients would be above the normal range. At the various hospitals and isolation centers, Figure 6 portends a green baseline colour predictive of the expected outcome after isolation and treatment. A restoration to point zero, normalization factor where the effects of the pandemic have become insignificant.

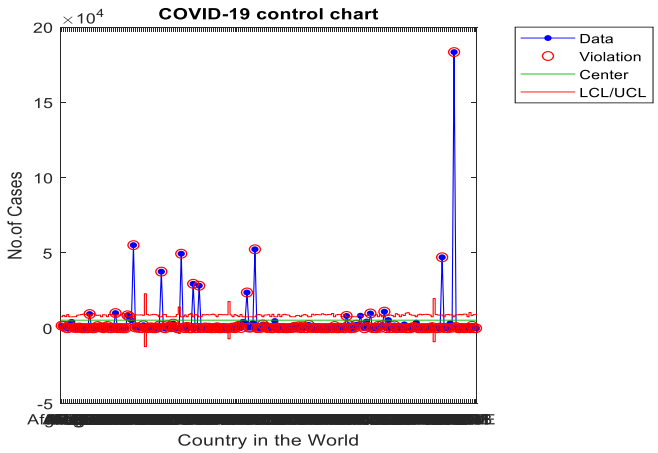

Figure 6: Software analysis of control charts of fifty countries with COVID-19 cases

Use of ultrasound as a therapy against COVID-19 viral; attack is a prognosis for future treatment from Equation 20. Acoustic waves are directed to the viral high energy pain ridden respiratory tracts, where the energy stimulates repairs and regeneration of damages. This would be particularly useful in patients with underlying health conditions as described in Equation 13. The characteristic pressure jump, irregularity and high amplitude is a diagnostic prescription which targeted at any viral target, should cause annihilation [12-17]. This is akin

to a projectile's motion, causing energy by compressing air molecules as it transmits from its source to the viral targets.

Conclusion and Recommendations

The following solutions are prescribed for subsequent viral attacks from a Physics perspective

1. Restore system to zero by vaccination: We propose a spatial normalization factor I +S=1, where I represents the infection, S denotes $(1-\varepsilon_k)$. An organic penicillin,containing spray-like virus inoculum deposited along the human respiratory tract capable of engulfing the virus is a proposition. This would weaken the virus and be a function that depends on time and depth, *V(x,t)* [18-19].
2. Heat shock treatments: Locating the viral infection and encircling the area with heat higher than the viral optimal temperature, $\frac{dT}{dt} > 0$, of the viral system will kill the viruses directly. However, the outcome of these interactions may be difficult to predict due to susceptibility and sensitivity effect of virus temperature on the host and pathogen species [20-21]. Our results show that changes in temperature may change the likelihood of pathogens successfully infecting certain species, which does not eliminate the possibility of resistant species being the most susceptible to a novel pathogen.
3. Sonic therapy: Another recommendation in the form of the use of pulsed ultrasound waves, to treat viral infected area successfully navigates barriers, and is vouched toxin-proof in nature. The ultrasound with acceleration ($a > a_{v;} \frac{dv}{dt}$), bursts through the viral shell of SARS-CoV-2. It creates $\Delta P_v$and outruns the virus, the sonic waves spread out and results in a sonic boom causing the virus to explode [22] as represented in Equation 13.

Acknowledgement

The authors wish to appreciate the publication support received from Covenant University, Nigeria.

References

1. Huang C, Wang Y, Li X, et al. Clinical features of patients infected with 2019 novel coronavirus in Wuhan, China. *Lancet*. 2020; 395(10223): 497- 506.
2. Pan Y, Guan H, Zhou S, et al. Initial CT findings and temporal changes in patients with the novel coronavirus pneumonia (2019-nCoV): a study of 63 patients in Wuhan, China. *EurRadiol*. 2020.
3. Okolo P. N., Onoja, A. Modelling COVID 19 Epidemics: The Role of Social Distancing and Isolation. Covenant Journal of Physical & Life Sciences. Covenant Journal of Physical and Life Sciences, 9, 1, 2021.

4. Zhou B, Li Y, Speer SD, Subba A, Lin X, Wentworth DE. Engineering temperature sensitive live attenuated influenza vaccines from emerging viruses. Vaccine. 30, 24:3691-3702, 2012.
5. Akinduti P. Akinniyi, Obafemi Y. Dorcas, Oranusi S Uche A. Sero-epidemiological Impact of SARS-Cov2 on Socio-Demographic Status of African Populace. Covenant Journal of Physical and Life Scieces, 8, 2, 2020.
6. Bernheim A, Mei X, Huang M, et al. Chest CT findings in coronavirus disease-19 (COVID-19): relationship to duration of infection. *Radiology*, 2020.
7. Johnston S. Impact of viruses on airway diseases. Eur.Respir. Rev. 2005;14(95):57-61.
8. Li, Q., Guan, X., Wu, P., Wang, X., Zhou, L., Tong, Y. Early transmission dynamics in Wuhan, China, of novel coronavirus – Infected pneumonia. *New England Journal of Medicine*, 2020.
9. Lu, H., Stratton, C. W., Tang, Y. Outbreak of pneumonia of unknown etiology in Wuhan, China: The mystery and the miracle. *Journal of Medical Virology*, 2020, 92, 401–402.
10. Huang, C., Wang, Y., Li, X., Ren, L., Zhao, J., Hu, Y., Zhang, L., Fan, G., Xu, J., Gu, X., Cheng, Z., Yu, T., Xia, J., Wei, Y., Wu, W., Xie, X., Yin, W., Li, H., Liu, M., Cao, B. Clinical features of patients infected with 2019 novel coronavirus in Wuhan, China. *The Lancet* 2020, 395, 497–506.
11. Siddharta, A., Pfaender S., Malassa A., Doerrbecker J., Anggakusuma, E. M., Nugraha, B., Steinmann, J., Todt, D., Vondran, F.W., Mateu-Gelabert, P., Goffinet, C., Steinmann, E. Inactivation of HCV and HIV by microwave: a novel approach for prevention of virus transmission among people who inject drugs. *Scientific Reports*, 2016, 6, 36619.
12. Sun, C.K., Tsai, Y.C., Chen, Y.J., Liu, T.M., Chen, H.Y., Wang, H.C., Lo, C.F. Resonant Dipolar Coupling of Microwaves with Confined Acoustic Vibrations in a Rod-shaped Virus. *Scientific Reports*, 2017, 7: 4611.
13. Jones, B.A., Lessler, J., Bianco, S., Kaufman J.H. Statistical Mechanics and Thermodynamics of Viral Evolution. *PLoS ONE*, 2015, 10(9): e0137482.
14. Ito, S., Stochastic thermodynamic interpretation of information geometry. *Physical review letters*, 2018, 121 (3), 030605.
15. Dehmer, M., Emmert-Streib, F., Chen, Z., Li, X., Shi, Y., Mathematical foundations and applications of graph entropy, 2016, Wiley-VCH.
16. Mau, J. Dynamics that underlie concepts of entropy. *AIP Conference Proceedings*, 2019, 2140, 020044.
17. Schulte, M.B., Draghi, J.A., Plotkin, J.B, Andino, R. Experimentally guided models reveal replication principles that shape the mutation distribution of RNA viruses. *eLife*, 2015; 4: e03753.09
18. Hadden, J.A., Perilla, J.R., Schlicksup, C.J., Venkatakrishnan, B., Zlotnick, A. Schulten, K. All-atom molecular dynamics of the HBV capsid reveals insights into biological function and cryo-EM resolution limits. *Elife*, 2018, 7, e32478.

19. Zitzmann, C., Kaderali, L. Mathematical Analysis of Viral Replication Dynamics and Antiviral Treatment Strategies: From Basic Models to Age-Based Multi-Scale Modeling. *Front Microbiol*. 2018, 9, 1546.
20. Quirouette, C., Younis, N.P., Reddy, M.B., Beauchemin, C.A. A mathematical model describing the localization and spread of influenza A virus infection within the human respiratory tract. Plos Computational Biology, 2020, 16(4): e1007705.
21. Pavić, M., Ruggeri, T., Simić, S. Maximum entropy principle for rarefied polyatomic gases. *Physica A*: Statistical Mechanics and its Applications, 2013, 392 (6), 1302-1317.
22. Marinova, M., Rauch, M., Mücke, M., Rolke, R., Gonzalez-Carmona, M.A., Henseler, J., Cuhls, H., Radbruch, L., Strassburg, C.P., Zhang, L., Schild, H.H., Strunk, H.M. High-intensity focused ultrasound (HIFU) for pancreatic carcinoma: evaluation of feasibility, reduction of tumour volume and pain intensity. *Eur. Radiol* 2016, 26, 4047–4056.